Sains Malaysiana 54(7)(2025): 1657-1666
*http://doi.org/10.17576/jsm-2025-5407-01*

# Systematic Approach to Boulder Stability Assessment at a Boulder Covered Area: Case Study at Gunung Bujang Melaka, Kampar, Perak

(Pendekatan Sistematik untuk Penilaian Kestabilan Tongkol di Kawasan Tongkol Tertutup: Kajian Kes di Gunung Bujang Melaka, Kampar, Perak)

TAN JIA QI[1], NORASIAH SULAIMAN[1], NOR SHAHIDAH MOHD NAZER[1], MUHAMMAD TAQIUDDIN ZAKARIA[1], NURUL 'AMALINA MD NOR[2], ASKURY ABD KADIR, ABDUL GHANI RAFEK[3], AILIE SOFYIANA SERASA[1], LEE KHAI ERN[4] & GOH THIAN LAI[1,*]

[1]*Department of Earth Sciences and Environment, Faculty of Science and Technology, Universiti Kebangsaan Malaysia, 43600 Bangi, Selangor, Malaysia*
[2]*Jabatan Mineral dan Geosains Malaysia, Perak, Jalan Sultan Azlan Shah, 31400 Ipoh, Perak, Malaysia*
[3]*Engineering Geology Advisory, 11, SS21/12, Damansara Utama, 47400 Petaling Jaya, Selangor, Malaysia*
[4]*Institute for Environment and Development (LESTARI), Universiti Kebangsaan Malaysia, 43600 UKM Bangi, Selangor, Malaysia*

*Received: 6 December 2024/Accepted: 26 May 2025*

ABSTRACT

Gunung Bujang Melaka is set to be developed into a tourist attraction, prompting a study of the granite boulders in the area to ensure visitor safety. This paper aimed to identify potential unstable boulders and produce a stability zonation map of the designated area. Aerial photogrammetry was conducted to create a 3D model of the project area, capturing the boulders' characteristics. Each boulder was delineated using 3D processing software-ShapeMetrix-to acquire dimensions, base dipping angles, and azimuths. The general slope angle of the project area was generated using the moving average grid method on the digital elevation model (DEM) produced from the 3D model. Tilt tests were performed on-site, showing a basic frictional angle of 30° and a peak frictional angle of 66°. Over 1,600 boulders were identified across the area, with 274 boulders having visible base angles evaluated using kinematic analysis and the Hoek & Bray block model for stability assessment. The results indicated five types of boulder stability: Exceptionally Stable (8, 3%), Very Stable (102, 37%), Stable (16, 6%), Likely Stable (126, 46%) and Potential Sliding (22, 8%). The remaining boulders, with their base planes concealed by surrounding boulders, were considered interlocking due to deep-seated and support from adjacent boulders. Mitigation measures such as bracing and anchoring are recommended based on their modes of failure.

Keywords: Boulder stability; drone photography; GIS processing; Hoek and Bray; kinematic analysis

ABSTRAK

Gunung Bujang Melaka yang akan dibangunkan sebagai tarikan pelancongan mencetuskan kajian terhadap tongkol granit di kawasan ini bagi memastikan keselamatan pelawat. Kajian ini bertujuan mengenalpasti kestabilan tongkol dan menghasilkan peta zonasi kestabilan untuk kawasan tersebut. Fotogrametri udara telah dijalankan untuk menghasilkan model 3D kawasan kajian bagi mencirikan setiap tongkol yang sedia ada. Setiap tongkol dilakarkan dengan penggunaan perisian pemprosesan 3D ShapeMetrix untuk memperoleh dimensi, sudut tapak dan arah kemiringan tongkol. Sudut cerun umum kawasan projek dijana menggunakan kaedah Moving Average atas Digital Elevation Model (DEM) yang dihasilkan daripada model 3D. Ujian kemiringan yang dijalankan menunjukkan sudut geseran asas adalah sebanyak 30° dan sudut geseran puncak adalah sebanyak 66°. Lebih daripada 1,600 bongkah telah dikenalpastikan di dalam kawasan kajian dan hanya 274 bongkah yang mempunyai tapak tongkol yang boleh dinilai maka dapat menggunakan analisis kinematik dan model blok Hoek & Bray untuk penilaian kestabilan mereka. Hasil tersebut mengelaskan kestabilan bongkah kepada lima kategori iaitu paling stabil (8 bongkah, 3%), sangat stabil(102 bongkah, 37%), stabil (16 bongkah, 6%), kemungkinan stabil (126 bongkah, 46%) dan berpotensi gelinciran (22 bongkah, 8%). Tongkol-tongkol yang mempunyai tapak kemiringan yang tersembunyi oleh tongkol sekeliling adalah dikelaskan kepada saling pancaan disebabkan kedudukan yan mendalam serta sokongan daripada bongkah bersebelahan. Langkah mitigasi seperti pendakap dan sauh dicadangkan berdasarkan mod kegagalan masing masing.

Kata kunci: Analisis kinematik; fotografi dron; Hoek dan Bray; kestabilan batu; pemprosesan GIS

## INTRODUCTION

Thousands of granite boulders, noted for their large-scale rillenkarren formations (Figure 1), cover the western slopes of Gunung Bujang Melaka, attracting numerous tourists. Despite their equilibrium state, the stacked boulders pose a potential hazard to visitors due to concerns over their long-term stability. The lack of established techniques for assessing the stability of large boulder accumulations necessitates this study. Most previous studies (Alejano & Carranza-Torres 2011; Alejano et al. 2022, 2010; Armesto et al. 2009; Pérez-Rey et al. 2019; Vann, Olaiz & Zapata 2019) have focused on individual precarious boulders, which are impractical for areas with plethora amount boulders. For instance, prior methods involved detailed surveys using Terrestrial Laser Scanning (TLS) and drones with Lidar to capture high-resolution 3D models of individual boulders, allowing for accurate analysis of their centers of gravity and potential failure risks (Alejano et al. 2017). However, these approaches are time-consuming and costly, making them unsuitable for regions with thousands of boulders. Therefore, this paper aims to establish an efficient and systematic method for evaluating boulder stability, creating a geohazard map, and recommending mitigation strategies for potentially unstable boulders.

## GEOLOGICAL SETTING

Gunung Bujang Melaka is part of the Main Range batholith and underlain by granite (Hutchison & Tan 2009). Based on the contour map generated from USGS Digital Elevation Map (2010), the slope dips westward and suggested to be windward slope due to its gentler slope gradient compared to the opposite slope (Figure 3(a)). The presence of rillenkarren formations - grooves cut into sloping and vertical rock surfaces and mostly reported from humid tropical environments (Migon' 2006), may be due to these topographical conditions. The granite in this area is predominantly porphyritic (Figure 2), consistent with the Main Range's geology (Hutchison & Tan 2009).

The site is situated on the foot slope of Gunung Bujang Melaka, near the Loji Rawatan Air Sungai Kampar reservoir (Figure 3(b)). It is accessible via Route A119, with the final approach involving a tarred road followed by an off-road section at Jeram, Perak. A natural stream flows beneath the boulders near the quarters where the owner's workers reside.

## AERIAL PHOTOGRAMMETRY

Three ground control points were established using a total station and permanent structures to determine the relative x, y, and z coordinates of the area, ensuring precise alignment with real-world coordinates before drone photography (Figure 4). The drone photographs were captured using a Phantom 4 V2 Pro at an elevation of 100 m above ground level (AGL), with the launch platform located near the quarter. The AGL was determined by evaluating the tallest obstacle in the area - a tree with a height of 70 m - and incorporating a 30 m buffer zone to avoid any unforeseen obstacles. Automated piloting was employed to capture images at regular intervals in an intersecting grid pattern. The camera was tilted at 60°, and 70% side and front overlaps were set to ensure comprehensive coverage of the area from various perspectives.

The captured images were then imported into an image processing software called ShapeMetrix, which constructs 3D models objects (boulders) in the images. This allows for the visualization of the 3D structure of each boulder and the identification of their base orientations, especially where they make physical contact with underneath boulders. Additionally, ShapeMetrix enables the measurement of the longest width and tallest height of each boulder with high accuracy.

## GIS PROCESSING

To calculate the area occupied by each boulder, a GIS tool was used to manually draw the boundaries of each surface boulder after importing the orthomosaic generated by ShapeMetrix. The area of each polygon was extracted, and further statistical analysis was conducted on the mean value of all the boulders' areas. The general topography of the area, represented by a Digital Elevation Model (DEM), was produced using the GRID method with a moving average. The radius of the search ellipse was set to three times the mean boulder area to account for the spatial relationship between adjacent boulders. Additionally, slope and aspect analyses were performed to determine the general slope angle and the direction of the topography where the boulders rest upon.

## ON-SITE JRC INVESTIGATION

A Barton comb (Figure 5(a)) was used on the surface of the boulders to trace their roughness. The profiles obtained from the Barton comb were compared with the Barton and Choubey (1977) chart to determine the Joint Roughness Coefficient (JRC), which is an essential parameter for determining friction angles.

## TILT TEST METHOD

The setup for the tilt test is illustrated in Figure 5(b). A rock specimen, halved or cut, is placed on a tilting platform with the sawn surfaces facing each other in a stacked configuration. The initial angle of the sawn surface ($\Theta_0$) is measured and recorded using a clinometer while the platform remains level. To prevent the lower block from sliding during the tilt, it is secured to the platform using plasticine. As the platform is manually tilted, the angle ($\Theta_p$) is recorded when the upper specimen either slides, topples, or slides followed by toppling. The basic friction angle ($\varphi$) is determined by adding $\Theta_0$ and $\Theta_p$.

FIGURE 1. Rillenkarren formation on granite boulders at Gunung Bujang Melaka

FIGURE 2. Granite boulders at the project area with porphyritic feature

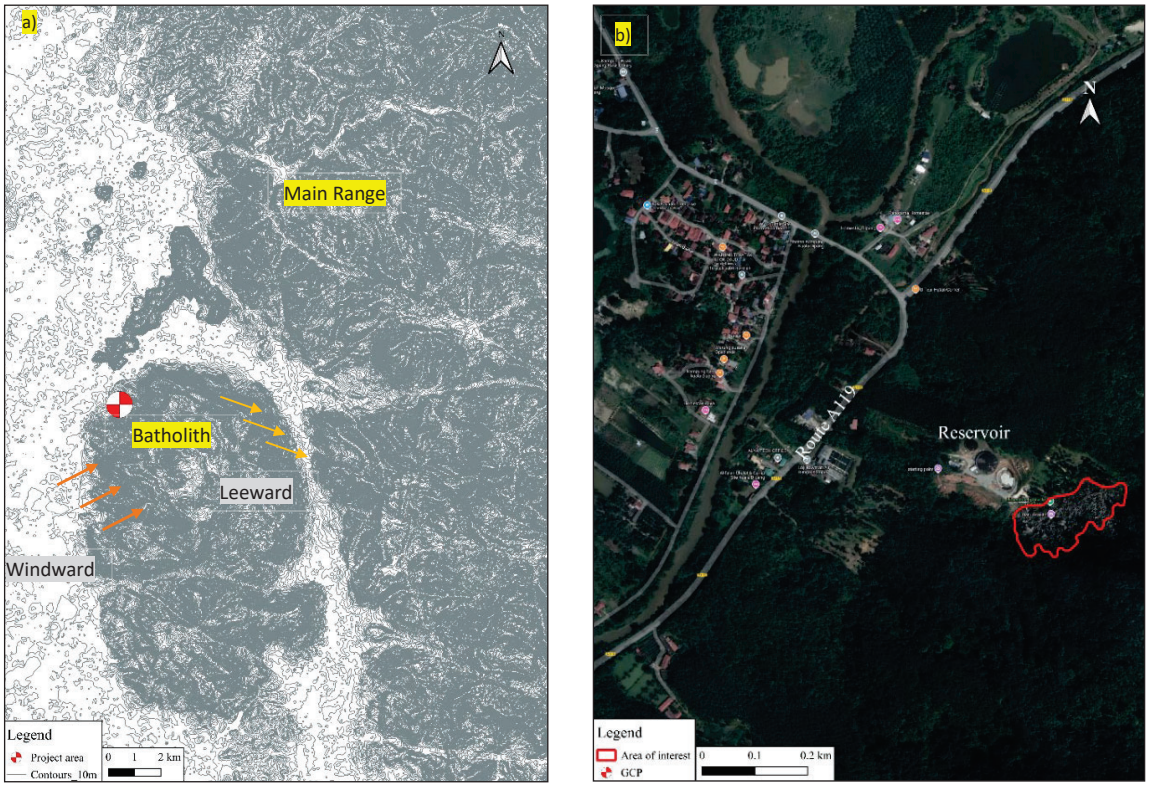


FIGURE 3. a) Regional contour map showing the windward and leeward slope and b) Location plan of the project area


FIGURE 4: i) GCP marker mat, ii) Total station setting up, and iii) Drone setting up


FIGURE 5. a) Example of Barton Comb with boulder's surface roughness profile and b) Example of tilt test

## HOEK AND BRAY CURVE METHOD

Boulder stability is primarily determined by the width-to-height ratio and the base angle of the boulders, as illustrated in the schematic diagram by Wyllie and Mah (2005) shown in Figure 6(a). During the tilt test, the dimensions of the block were also measured and recorded, including the width of the base of the sawn surface (W) of the upper rock specimen, which is parallel to the tilting platform, and the maximum height (H) of the block. The width-to-height (W:H) ratio was then plotted against the corresponding tilt angle ($\Theta_p$) to assess the mode of failure. The Hoek and Bray curve, along with the base plane angle of failure (represented by a vertical line), was delineated on the plot. The results were classified into four mutually exclusive categories: Stable (STA), slide (SL), topple (T), and slide followed by topple (SFT), specific to the project area (Figure 7).

The threshold for the highest degree of failure potential was governed by the peak friction angle of the boulders, with the JRC values acquired in the field used as inputs for the calculation based on formula (1) suggested by Goh, Ghani Rafek and Hariri Arifin (2014).

$$\phi_p = -0.087\text{JRC}^2 + 4.32\text{JRC} + 34.1 \quad (1)$$

## KINEMATIC ANALYSIS METHOD

The Hoek and Bray model can assess the stability of a boulder based on its geometry but does not account for whether the boulder is susceptible to falling, as the direction of movement is a critical governing factor. Therefore, kinematic analysis is used to evaluate whether the direction of potential movement is feasible or constrained. The closely packed arrangement of boulders forms a rock mass, further justifying the application of kinematic analysis.

According to Wyllie and Mah (2005), the rule of thumb for kinematic analysis is straightforward: for sliding to occur, the following conditions must be met for the base plane angle of the boulder: i) steeper than friction angle (φ), and ii). Falls within ± 20° of the dipping direction of the general slope.

Kinematic analysis for toppling of boulders is impractical because it suggests that the base plane of the boulder must dip in a direction almost or directly opposite to the slope. However, this orientation would increase the boulder's stability rather than induce failure. In such cases, the projection of the boulder's center of gravity extends inward, into the slope, with the opposite base plane provides support, preventing toppling.

## RESULT ON PHOTOGRAMMETRY AND GIS

Figure 8(a) shows the orthomosaic of the project area, generated using ShapeMetrix. The total area of interest is 17,197.4 m² (equivalent to 4.25 acres), containing 1,604 boulders. A statistical analysis using GIS showed that the areas of individual boulders range from 0.19 m² to 167.6 m², with a mean value of 2.85 m². The first quartile is 1.85 m², the third quartile is 8.34 m², and the interquartile range is 6.49 m².

However, only 274 boulders were eligible for further analysis, as the bases of the remaining boulders were not exposed, preventing a full evaluation. These boulders are considered interlocking due to being deep-seated and interlocked with adjacent boulders, which provide additional support. The bases of the 274 boulders were delineated using ShapeMetrix, which enabled the identification of their base planes and dimensions (width and height). Table 1 summarizes the key findings on the dimension of the boulders in the area.

## JRC RESULT

A total of 22 readings were collected in the field. The majority of the Barton comb profiles (Figure 6(b)) indicated that the JRC values for the boulders fell within the 8-10 range, with some readings in the 10-12 and 12-14

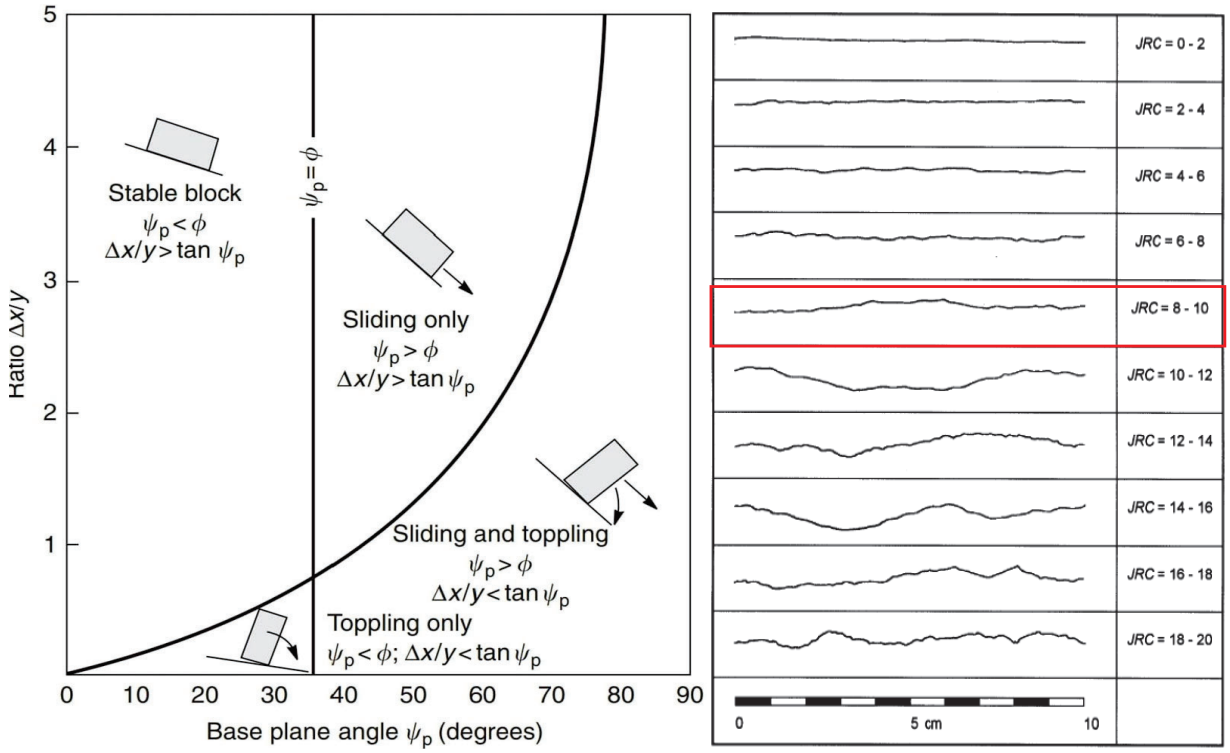


FIGURE 6. a) Hoek and Bray graph showing different modes of failure in certain base plane angle (Hoek & Bray 1977) and b) Surface roughness profile with their respective JRC value (Barton & Choubey 1977)

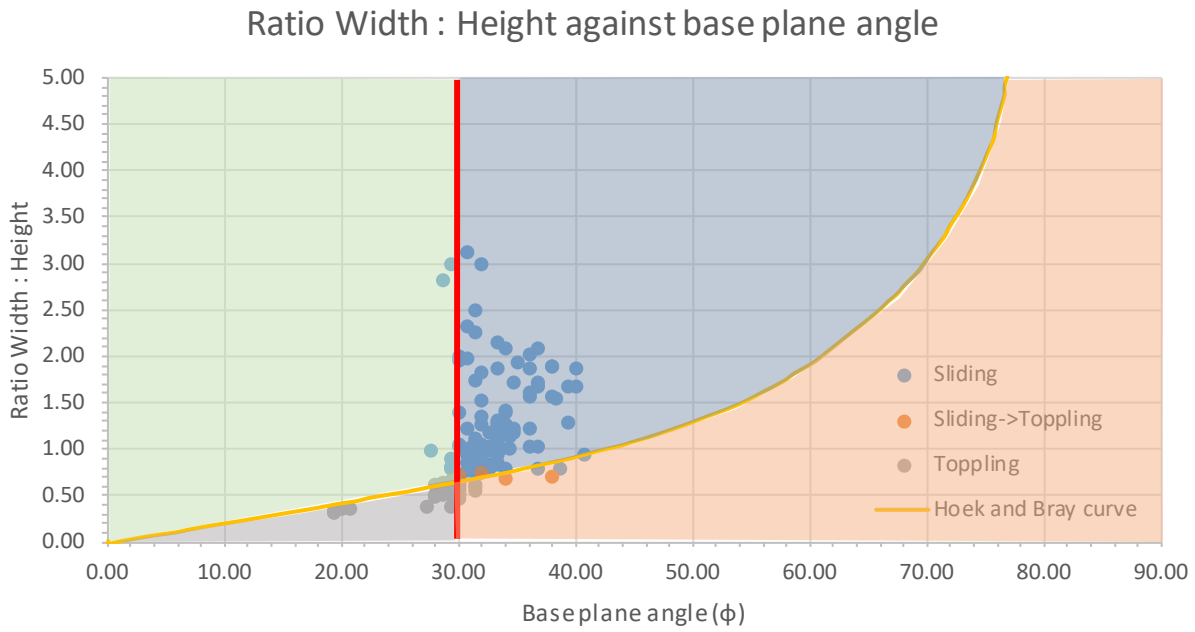


FIGURE 7. Tilt test graphical result with Hoek and Bray classification

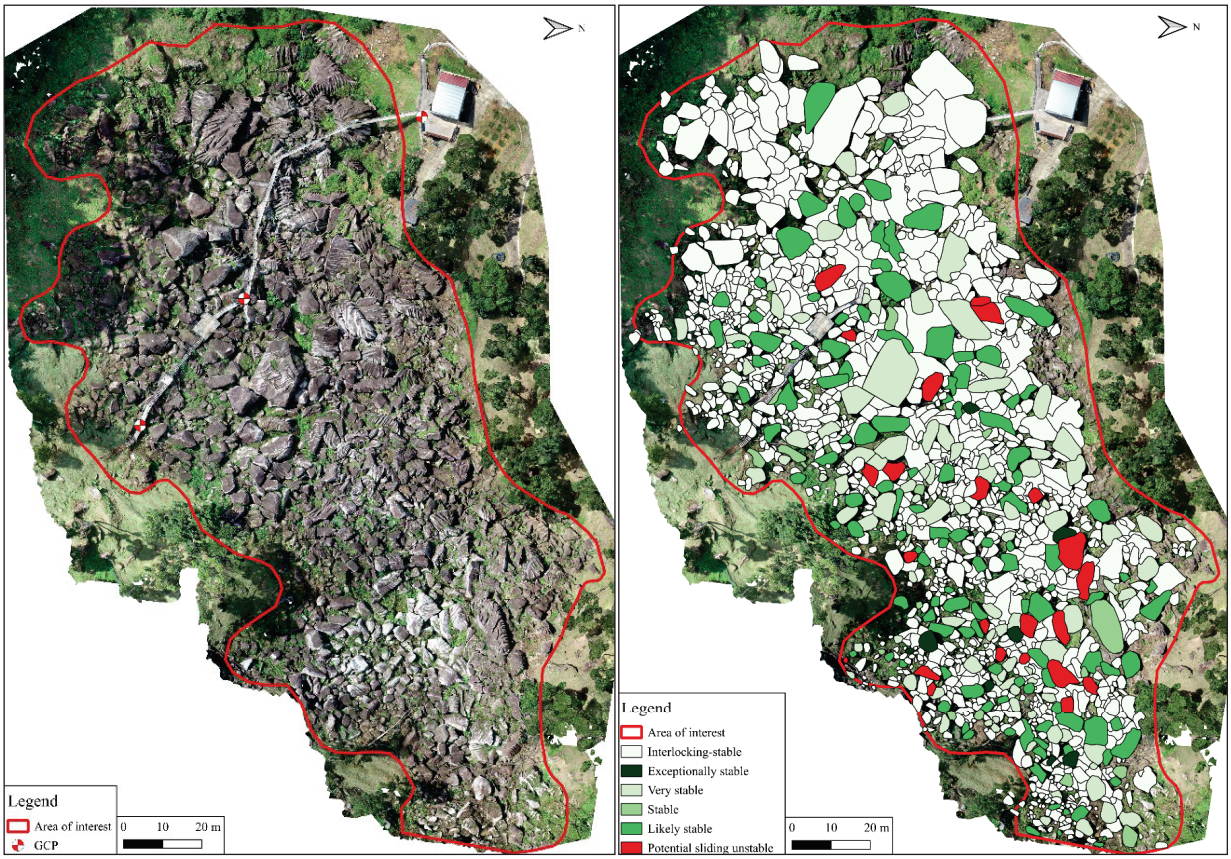


FIGURE 8. a) Orthomosaic image of project area and b) Geohazard map of the project area

TABLE 1. Summary of the boulders' dimension at the project area

| Description | Value | Boulder ID |
|---|---|---|
| Largest boulder | 20.39 m | C79 |
| Smallest boulder | 0.78 m | C95 |
| Tallest boulder | 8.61 m | B54 |
| Shortest boulder | 0.30 m | C45 |
| Steepest base plane angle | 73.78° | A12 |
| Gentlest base plane angle | 2.14° | B9 |
| Highest W:H ratio | 10.82 | B67 |
| Lowest W:H ratio | 0.36 | C20 |

categories. Consequently, a JRC value of 10 was used in formula 2.1, resulting in an upper limit for the peak friction angle of 66°.

## HOEK AND BRAY RESULT

A total of 130 angles of failure readings were obtained from the tilt test, with corresponding width and height measurements for each sample. These readings were plotted on a graph to represent different failure modes (Figure 9(b)). According to Wyllie and Mah (2005), the minimum angles for sliding failure, sliding followed by toppling, and maximum toppling failure are initially similar. However, tilt test results show that the minimum angle for sliding failure is 28°, with a width-to-height (W:H) ratio of 1. For sliding followed by toppling, the minimum angle is 30°, with W:H ratios ranging from 0.63 to 0.72. The maximum toppling failure angle is 32°, with W:H ratios ranging from 0.54 to 0.61. To simplify the use of the graph, these three angles were

averaged, resulting in a value of 30°, represented by the red line. The Hoek and Bray curve (Wyllie & Mah 2005) fit well with the plotted data.

Using this approach, the failure mode of each eligible boulder was determined based on its base angle and W:H ratio (Figure 9). Out of the 274 boulders analyzed, 125 were classified as stable, 141 showed potential for sliding, 8 had potential for sliding followed by toppling, and none exhibited pure toppling potential. A boulder is considered high risk of sliding or sliding followed by toppling if its base plane angle exceeds 66°. In this study, 1 boulder was identified as having a high risk of sliding, and 3 boulders were classified as having a high risk of sliding followed by toppling.

## KINEMATIC ANALYSIS RESULT

The analysis of 274 boulders shows that 252 are stable, while 22 exhibit potential instability due to sliding, assuming a friction angle of 30° based on lab results. Among the 251 stable boulders, 126 (likely stable) have base plane angles steeper than the general slope, with a relative azimuth difference of more than 20° between the base plane and the slope direction. Additionally, 16 boulders (stable) have gentler base plane angles compared to the general slope, but their azimuth difference is less than 20°. The remaining 102 boulders (very stable) have base planes gentler than both the friction angle and the general slope angle, with a relative azimuth difference of more than 20°. Also, 8 boulders have their base plane angles dipping into the slope, categorizing them as exceptionally stable.

## GEOHAZARD

The assumption that boulders meeting the criteria such as deep-seated, with lateral support by adjacent boulders, and base-invisible are considered interlocking-stable was combined with kinematic analysis and the Hoek & Bray method to produce a geohazard map of the project area (Figure 8(b)). The map shows a few potential failure boulders randomly distributed across the site, covering only 1.4% of the total area (241 m², or 0.06 acres) and only sliding potential (SL) is identified across the boulders. Table 2 summarized the potential failure boulder based on their characteristic.

## DISCUSSION

The Hoek & Bray method identified more boulders as unstable compared to the kinematic analysis, which is likely due to the fact that Hoek & Bray does not account for azimuthal variations in base plane orientation. Kinematic analysis, which incorporates azimuth as a key factor, provides a more comprehensive assessment of the potential for boulder failure. However, the Hoek & Bray model is more effective in classifying different failure modes, such as sliding versus sliding followed by toppling, which is useful for informing mitigation strategies. However, none of the boulders classified as having sliding potential through kinematic analysis are determined to have either sliding followed by toppling or toppling potential through the Hoek & Bray model.

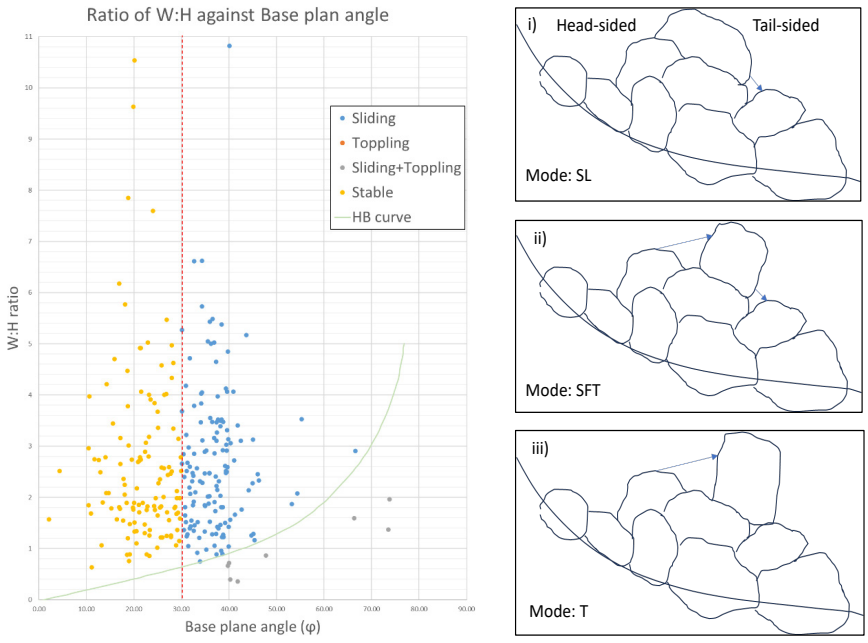


FIGURE 9. a) Graphical result of boulder's mode of failure based on Hoek and Bray classification and b) Schematic diagrams of mitigation on different modes of failure (arrow pointing upward represents anchor while arrow pointing downward represent brace)

TABLE 2. Summary of the boulders' failure mode at the project area

| Description | Value | Failure mode | Boulder ID |
|---|---|---|---|
| Longest boulder | 11.36 m | SL | B63 |
| Smallest boulder | 1.08 m | SL | C2 |
| Tallest boulder | 3.63 m | SL | C64 |
| Shortest boulder | 0.76 m | SL | B37 |
| Highest W:H ratio | 4.64 | SL | B40 |
| Lowest W:H ratio | 0.92 | SL | C2 |

## CONCLUSION AND LIMITATION

The overall stability of the study area is deemed adequate, with only a small number of boulders requiring mitigation. Given the scattered nature of problematic boulders, avoidance is a feasible strategy for future development. However, mitigation measures such as anchors or braces should be implemented for boulders at risk of failure to enhance their stability. The placement of these supports is crucial and depends on the mode of failure (Figure 9(b)).

For sliding boulders (SL), braces should be positioned at the tail to provide additional lateral support to the base. For toppling boulders (T), anchors should be placed at the head to counteract the toppling force. For sliding followed by toppling (SFT), braces should be located at the tail to prevent sliding, while anchors should be placed at the head to pull back the boulder and prevent toppling. Both tail-bracing and head-anchoring work together to form a larger, pseudo boulder with enhanced base support.

The angle of tail-bracing depends on the availability of a tail-boulder adjacent to the potential failure boulder's tail. Ideally, the brace should be aligned at the same angle or at a downward angle relative to the sliding axis of the boulder to maximize support. Similarly, the angle of head-anchoring depends on the availability of a head-boulder adjacent to the potential failure boulder's head. The anchor should be placed on the head side of the boulder, higher than its center of gravity, and anchored to the adjacent head-boulder. The anchor angle should be parallel or downward relative to the direction of toppling to provide optimal stabilization.

The primary limitation of this study is the assumption of simple 2D boulder geometry, which may not fully capture the irregular shapes and center-of-gravity calculations needed for a more accurate assessment. Additionally, boulders deep seated into the soil slope are not evaluated as they are beyond the limitation of the approach which only suitable for rock-rock analysis. Future research could benefit from using advanced computational models to better assess the stability of irregularly shaped boulders.

## ACKNOWLEDGMENTS

This research is also supported by Research Grant GUP-2023-022 and Subsurface Engineering Sdn Bhd. The co-operation of all parties and agencies in the success of this study is greatly appreciated.

## REFERENCES

Alejano, L.R. & Carranza-Torres, C. 2011. An empirical approach for estimating shear strength of decomposed granites in Galicia, Spain. *Engineering Geology* 120(1-4): 91-102. https://doi.org/10.1016/j.enggeo.2011.04.003

Alejano, L.R., Pérez-Rey, I., Muñiz Menéndez, M., Riquelme, A. & Walton, G. 2022. Considerations relevant to the stability of granite boulders. *Rock Mechanics and Rock Engineering* 55: 2729-2745. 10.1007/s00603-021-02525-9

Alejano, L.R., Muralha, J., Ulusay, R., Li, C.C., Pérez-Rey, I., Karakul, H., Chryssanthakis, P., Aydan, Ö., Martínez, J. & Zhang, N. 2017. A benchmark experiment to assess factors affecting tilt test results for sawcut rock surfaces. *Rock Mech. Rock Eng.* 50(9): 2547-2562

Alejano, L.R., Ordóñez, C., Armesto, J. & Rivas, T. 2010. Assessment of the instability hazard of a granite boulder. *Nat. Hazards* 53: 77-95. https://doi.org/10.1007/s11069-009-9413-0

Armesto, J., Ordóñez, C., Alejano, L. & Arias, P. 2009. Terrestrial laser scanning used to determine the geometry of a granite boulder for stability analysis purposes. *Geomorphology* 106(3-4): 271-277. https://doi.org/10.1016/j.geomorph.2008.11.005

Barton, N. & Choubey, V. 1977. The shear strength of rock joints in theory and practice. *Rock Mechanics* 10: 1-54. 10.1007/BF01261801

Goh, T.L., Ghani Rafek, A. & Hariri Arifin, M. 2014. Correlation of joint roughness coefficient with peak friction angles of discontinuity planes of granite, Peninsular Malaysia. *Sains Malaysiana* 43(5): 751-756.

Hoek, E. & Bray, J. 1977. *Rock Slope Engineering*, 1st ed. London: IMM.

Hutchison, C.S. & Tan, D.N.K. 2009. *Geology of Peninsular Malaysia*. Kuala Lumpur: University of Malaya and Geological Society of Malaysia.

Migon´, P. 2006. *Geomorphological Landscapes of the World*. Springer Dordrecht.

Pérez-Rey, I., Alejano, L.R., Riquelme, A. & González-deSantos, L. 2019. Failure mechanisms and stability analyses of granitic boulders focusing a case study in Galicia (Spain). *International Journal of Rock Mechanics and Mining Sciences* 119: 58-71. https://doi.org/10.1016/j.ijrmms.2019.04.009

Vann, J., Olaiz, A.H. & Zapata, C. 2019. A practical approach to a reliability-based stability evaluation of precariously balanced granite boulders. *53rd US Rock Mechanics/Geomechanics Symposium*, Brooklyn, New York.

Wyllie, D.C. & Mah, C.W. 2005. *Rock Slope Engineering: Civil and Mining*. 4th ed. London: Spon Press.

*Corresponding author; email: gdsbgoh@gmail.com